Environ. Sci. Technol. **2005**, *39,* 3245−3254

Optimization-Based Source Apportionment of $PM_{2.5}$ Incorporating Gas-to-Particle Ratios

AMIT MARMUR,* ALPER UNAL, JAMES A. MULHOLLAND, AND ARMISTEAD G. RUSSELL

School of Civil and Environmental Engineering, Georgia Institute of Technology, Atlanta, Georgia 30332-0512

A modified approach to $PM_{2.5}$ source apportionment is developed, using source indicative $SO_2/PM_{2.5}$, $CO/PM_{2.5}$, and $NO_x/PM_{2.5}$ ratios as constraints, in addition to the commonly used particulate-phase source profiles. Additional information from using gas-to-particle ratios assists in reducing collinearity between source profiles, a problem that often limits the source-identification capabilities and accuracy of traditional receptor models. This is especially true in the absence of speciated organic carbon measurements. In the approach presented here, the solution is based on a global optimization mechanism, minimizing the weighted error between apportioned and ambient levels of $PM_{2.5}$ components, while introducing constraints on calculated source contributions that ensure that the ambient gas-phase pollutants (SO_2, CO, and NO_y) are reasonable. This technique was applied to a 25-month dataset of daily $PM_{2.5}$ measurements (total mass and composition) at the Atlanta Jefferson Street SEARCH site. Results indicate that this technique was able to split the contributions of mobile sources (gasoline and diesel vehicles) more accurately than particulate-phase source apportionment methods. Furthermore, this technique was able to better quantify the direct contribution (primary $PM_{2.5}$) of coal-fired power plants to ambient $PM_{2.5}$ levels.

Introduction

Chemical mass balance (CMB) receptor models are a common tool for apportioning of ambient levels of pollutants (mainly particulate matter) among the major contributing sources. CMB combines the chemical and physical characteristics of particles or gases measured at sources and receptors to quantify the source contributions to the receptor. The quantification is based on the solution to a set of linear equations that express each receptor's ambient chemical concentration as a linear sum of products of source-profile abundances and source contributions (*1*, *2*), as expressed by

$$C_i = \sum_{j=1}^{n} f_{ij} S_j + e_i \qquad (1)$$

where C_i = ambient concentration of chemical species i ($\mu g/m^3$); $f_{i,j}$ = fraction of species i in emissions from source j; S_j = contribution (source strength) of source j ($\mu g/m^3$); n = total number of sources; and e_i = error term.

* Corresponding author phone: 404-385-4565; fax: 404-894-8266; e-mail: amit.marmur@ce.gatech.edu.

The source profile abundances (f_{ij}, the mass fraction of a chemical in the emissions from each source type) and the receptor concentrations (C_i), along with uncertainty estimates, serve as input data to the CMB model. The output consists of the contribution of each source category (S_j) to the measured concentration of different species at the receptor.

In CMB8 (2), the effective variance (EV) weighting for least squares calculations is applied, to find the best solution to the set of equations given by eq 1. The effective weighting method takes into account both the uncertainties in the ambient measurements and the uncertainties in the source-profile compositions. In practice, CMB8 performs a series of matrix operations to minimize χ^2, given as (*3*)

$$\chi^2 = \sum_{i=1}^{m} \frac{(C_i - \sum_{j=1}^{n} f_{ij} S_j)^2}{\sigma_{C_i}{}^2 + \sum_{j=1}^{n} \sigma_{fij}{}^2 S_j{}^2} \qquad (2)$$

where σ_{C_i} = one standard deviation precision of the C_i measurement; $\sigma_{f_{ij}}$ = one standard deviation of the f_{ij} measurement; and m = total number of species.

If the $\sigma_{f_{ij}}$ are set to zero, the solution reduces to the ordinary weighted least-squares (OWLS) solution (*3*), taking only the uncertainties in the ambient measurements into account.

CMB models are based on the following assumptions (*2*): (i) Compositions of source emissions are constant over the period of ambient and source sampling. (ii) Chemical species do not react with each other, i.e., they add linearly. (iii) All sources with a potential for significantly contributing to the receptor are included in the analysis. (iv) The source compositions are linearly independent of each other. (v) The number of sources or source categories is less than or equal to the number of chemical species. (vi) Measurement uncertainties are random, uncorrelated, and normally distributed.

Of these, one of the major assumptions limiting the ability of CMB models to identify and quantitatively provide impacts of the major sources is the linear independence of source profiles, when those profiles are based solely on traditional species. For apportionment of $PM_{2.5}$ (particulate matter with a diameter less than 2.5 μm), source profiles including major ions (SO_4^{-2}, NO_3^-, NH_4^+, Cl^-), elemental and organic carbon fractions (EC, OC), and trace metals are typically used. Some source categories share relatively similar profiles (e.g., diesel and gasoline vehicles), limiting the ability of CMB to accurately and consistently apportion the PM mass between those sources, particularly in the presence of other sources of OC and EC. To address this issue, recent source-apportionment studies make use of speciated organic compounds ("organic markers") to apportion OC (*4*−*6*), a major component in emissions from mobile sources, vegetative burning, and meat charbroiling. However, some sources share organic markers (e.g., hopanes and steranes in both gasoline and diesel vehicles), making it difficult to accurately and consistently apportion the OC mass between those sources. In addition, speciated ambient OC data are not yet commonly available.

Model Description

Incorporating Gas-to-Particle Ratios in $PM_{2.5}$ Source-Apportionment. Here we apply an extended CMB approach for $PM_{2.5}$ source-apportionment which incorporates source-

10.1021/es0490121 CCC: $30.25
Published on Web 03/29/2005

indicative $SO_2/PM_{2.5}$, $CO/PM_{2.5}$, and $NO_x/PM_{2.5}$ ratios, in addition to the commonly used $PM_{2.5}$ source profiles. Such ratios, along with ambient gas-phase data, can further assist in identifying sources, as sources that may have fairly similar $PM_{2.5}$ emissions may have significantly different gaseous emissions. Such gas-to-particle ratios may vary during transport from source to receptor, due to different deposition rates and reactivity. However, the atmospheric lifetimes of SO_2 (about a week), CO (1−4 months), and NO_x (1−7 days) (*7*) are long enough to assume that no major change in the gas-to-particle ratio will occur within an urban to regional airshed, given that the typical lifetime of a fine particle is in the order of days to weeks, as well (*8*). Even so, variations in the gas-to-particle ratios, along with uncertainties in the initial estimate used, need to be considered.

A few studies have shown the increased resolution in source apportionment of two-phase receptor models (*9*−*13*), though this is not a common practice in the source apportionment literature. Applying a two-phase receptor model for PM_{10} and nonmethane-hydrocarbons (NMHC) has shown to significantly reduce the collinearity problem (*9*). A study dealing with decay-adjusted receptor modeling (*13*) has shown small improvements in the agreement between CMB-predicted and observed concentrations of individual VOCs, but did not significantly change the estimated emissions contributions. These studies made use of two-phase source profiles in which the profile included the fractional composition of both PM and gas-phase data (speciated VOC, NO_x, SO_2, and CO) in a single profile, and χ^2 was minimized based on all these species. However, when eq 1 is solved in this manner, several issues arise. First, since these gas-phase species are reactive, the numerator in χ^2 cannot be simply expected to approach zero. In addition, the uncertainty in the measured ambient concentration is likely lower for major gas-phase species, compared to speciated $PM_{2.5}$ components. Hence, these major gaseous species are likely to drive the minimization of χ^2 (assuming uncertainties in the source profile compositions are comparable), despite the fact that for many sources of $PM_{2.5}$ the fraction of $PM_{2.5}$ emissions is much smaller than that of gas-phase emissions. For example, data from the national emission inventory for the United States (*14*) indicate that only about 0.6% of the total mass emissions from coal-fired power plants are $PM_{2.5}$, with the remaining and major part being gases (SO_2 and NO_x).

To avoid inaccuracies evolving from the use of two-phase source profiles and the straightforward minimization of χ^2 including gaseous species as fitting species, we suggest using ratios of $SO_2/PM_{2.5}$, $CO/PM_{2.5}$, and $NO_x/PM_{2.5}$ in emissions from the various sources to bound acceptable solutions to the source apportionment problem (eq 1), without directly including these data in the process of minimizing χ^2. That is, this information is used as a constraint, but not directly in the source profiles used by CMB. This information adds three constraint equations to the apportionment process, based on the same principles as in eq 1. The ambient SO_2 levels can then be expressed as

$$[SO_2] = \sum_{j=1}^{n} \left(\frac{SO_2}{PM_{2.5}}\right)_j S_j \qquad (3)$$

where: $[SO_2]$ = ambient SO_2 concentration ($\mu g/m^3$); $\left(\frac{SO_2}{PM_{2.5}}\right)_j$ = $SO_2/PM_{2.5}$ ratio in emissions from source j (mass/mass); S_j = contribution (source strength) of source j ($\mu g/m^3$) to the $PM_{2.5}$ loading; and n = total number of sources.

Similar equations can be expressed also for ambient CO and NO_x. Due to uncertainties in the initial estimate of the gas-to-particle ratio at the source, and to account for possible changes to these ratios during transport, we suggest using these equations (eq 3) to bound acceptable solutions to the $PM_{2.5}$ source-apportionment problem (eq 1), but not as part of the error minimization process. In practice, we suggest that such an acceptable solution is one that predicts the ambient SO_2, CO, and NO_x concentrations within a factor of 3 (under or over prediction) of the observed value (sensitivity to this factor is addressed shortly). Hence, the goal is to find an optimum solution based on the particulate-phase data, which adhere to somewhat more flexible constraints on the gaseous side.

Use of Global Optimization Models for Source-Apportionment. To solve the $PM_{2.5}$ source-apportionment problem (eq 1), subject to gas-phase constraints, we use a global optimization program. A large variety of quantitative decision problems in the applied sciences, engineering, and economics can be described by constrained optimization models. In these models, the best decision is sought that satisfies all stated feasibility constraints and maximizes (or minimizes) the value of a given objective function. The general mathematical form of these models is summarized as follows (*15*, *16*): (i) max $f(x)$; (ii) $a \le x \le b$; and (iii) $g(x) \le 0$ where x = a real n-vector (to describe feasible decisions); a,b = finite, component-wise vector bounds imposed on x; $f(x)$ = a continuous function (to describe the model objective); and $g(x)$ = a continuous vector function (to describe the model constraints; the inequality is interpreted component-wise).

The objective of global optimization is to find the best solution of nonlinear decision models in the possible presence of multiple locally optimal solutions. Here, LGO (Lipschitz(−continuous) global optimizer) is used (*15*, *16*). LGO integrates a suite of robust and efficient global and local scope solvers. These include the following: global adaptive partition and search (branch-and-bound); adaptive global random search; local (convex) unconstrained optimization; and local (convex) constrained optimization. The LGO implementation of these methods does not require derivative information. Their operations are based exclusively on the computation of the objective and constraint function values, at algorithmically selected search points.

Here, LGO was applied to identify and quantify the sources contributing to ambient levels of particulate matter. In practice, LGO was applied to solve the set of equations represented by eq 1 (22 eqs for 4 ions, 2 carbon fractions, and 16 trace metals), by setting χ^2 (eq 2) as the objective function to be minimized. The solution was set subject to the constraint that the total apportioned levels of SO_2, CO, and NO_x (as calculated by eq 3) lie within a factor of 3 of the observed ambient levels.

Model Implementation

Test Case: SEARCH 25-Month Dataset, Jefferson St., Atlanta, Georgia. To evaluate this modified approach for source-apportionment, we used the SEARCH (Southeastern Aerosol Research and Characterization) 25-month (8/98−8/00) dataset for the Jefferson St. (JST) site in Atlanta, GA (*17*, *18*), which included data on total $PM_{2.5}$ mass (gravimetric measure) and its components. The JST site is located 4 km northwest of downtown Atlanta in an industrial and commercial area. The main objectives of SEARCH include the understanding of composition and sources of PM in the southeast (*17*, *18*). SEARCH data are being used for the Aerosol Research Inhalation Epidemiological Study (ARIES) air-quality health study in Atlanta, GA (*17*), and one motivation of this work is to assess the possibility of using source information derived from receptor modeling in epidemiologic studies. For the speciation of $PM_{2.5}$, a manual, filter-based, particle composition monitor (PCM) was operated daily. The PCM included three channels to collect 24-h integrated samples for analysis of major ions, trace metals, and organic

TABLE 1. Mean, Standard Deviation, Minimum, and Maximum of Ambient Levels of the Species Used for the Source Apportionment, JST site, Atlanta, GA

	$\mu g/m^3$			
species	mean	SD	min	max
$PM_{2.5}$	19.1	8.9	1.9	54.6
SO_4^{-2}	5.41	3.65	0.53	20.8
NO_3^-	1.12	0.87	0.00	7.49
Cl^-	0.11	0.08	0.02	0.83
NH_4^+	2.79	1.60	0.30	10.3
EC	1.98	1.36	0.17	11.9
OC	4.46	2.21	0.66	18.4
Al	1.61×10^{-2}	4.52×10^{-2}	6.16×10^{-3}	9.00×10^{-1}
As	1.42×10^{-3}	1.35×10^{-3}	5.05×10^{-4}	1.51×10^{-2}
Ba	1.81×10^{-2}	8.01×10^{-3}	1.45×10^{-2}	5.69×10^{-2}
Br	4.04×10^{-3}	7.97×10^{-3}	2.60×10^{-4}	2.07×10^{-1}
Ca	5.37×10^{-2}	4.48×10^{-2}	4.04×10^{-3}	5.02×10^{-1}
Cu	3.70×10^{-3}	4.57×10^{-3}	6.15×10^{-4}	4.19×10^{-2}
Fe	8.92×10^{-2}	7.45×10^{-2}	5.34×10^{-3}	$1.05 \times 10^{+0}$
K	6.51×10^{-2}	5.86×10^{-2}	6.37×10^{-3}	8.27×10^{-1}
Mn	1.91×10^{-3}	1.54×10^{-3}	4.00×10^{-4}	1.31×10^{-2}
Pb	6.40×10^{-3}	7.49×10^{-3}	1.17×10^{-3}	7.83×10^{-2}
Sb	3.34×10^{-3}	4.40×10^{-3}	2.13×10^{-3}	1.07×10^{-1}
Se	1.32×10^{-3}	1.26×10^{-3}	3.50×10^{-4}	1.01×10^{-2}
Si	1.12×10^{-1}	1.15×10^{-1}	1.05×10^{-2}	$1.83 \times 10^{+0}$
Sn	4.32×10^{-3}	1.92×10^{-3}	3.53×10^{-3}	1.72×10^{-2}
Ti	4.78×10^{-3}	4.38×10^{-3}	2.14×10^{-3}	5.46×10^{-2}
Zn	1.63×10^{-2}	1.61×10^{-2}	4.23×10^{-4}	2.11×10^{-1}
SO_2	16.6	12.3	1.4	98.1
CO	560	423	180	4020
NO_y	108	68.2	12.4	590

and elemental carbon in $PM_{2.5}$ size range (*17*). Ion chromatography (IC) was used to quantify water-soluble ionic species. Elemental and organic carbon collected on quartz filters were measured by thermal optical reflectance (TOR). Trace metals were measured by X-ray fluorescence (XRF). Ambient values of daily SO_2, CO, and NO_y were reported as well. Mean values and standard deviations measured at the JST site for the species and time period (8/98−8/00) used in this analysis are given in Table 1. Note that NO_y was used rather than NO_x, to account for the amount of NO and NO_2 oxidized to other nitrogen forms, such as HNO_3 and peroxy acetyl nitrate (PAN). The average NO_x/NO_y mass ratio was 0.89, indicating "fresh" local emissions (compared to 0.63 at the rural Yorkville site, 55 km west northwest of Atlanta). The concentration values were used for the measured data, and the summation of the analytical uncertainty and $^1/_3$ of the detection limit value was used as the overall uncertainty assigned to each measured value (*18*). Values below the detection limit were replaced by half of the detection limit values, and their overall uncertainties were set at $^5/_6$ of the detection limit values (*18*). Missing values were replaced by the geometric mean of the measured values, and their accompanying uncertainties were set at 4 times this geometric mean value (*18*).

The major source categories used in the source apportionment included light-duty gasoline vehicles (LDGV), heavy-duty diesel vehicles (HDDV), fugitive soil dust (SDUST), vegetative burning (BURN), coal-fired power plants (CFPP), and cement kilns (CEM). To address the formation of secondary pollutants, we also included theoretical profiles based on the molecular weight fractions for ammonium sulfate (AMSULF), ammonium bisulfate (AMBSLF), ammonium nitrate (AMNIT), and secondary/other OC (OTHEROC). The secondary/other OC category will include any OC not apportioned to one of the primary source categories above. Of special note are emissions from meat charbroiling, dominated almost solely by OC emissions (*19*), with no unique inorganic marker, and characterized by low $SO_2/PM_{2.5}$ and $CO/PM_{2.5}$ ratios (*19*, *20*). This makes it very difficult to distinguish between emissions from meat charbroiling and secondary OC formation. For this reason, meat charbroiling emissions were not apportioned directly, but were rather lumped into the secondary/other OC category.

Source profiles used for LDGV and HDDV were based on measurements as part of the Northern Front Range Air Quality Study (NFRAQS) (*21*). The profiles used for vegetative burning, power plants, and cement kilns were based on measurements done as part of the Big Bend Regional Aerosol Visibility and Observational (BRAVO) study (*19*). The soil dust profile used was from more regionally representative measurements in Alabama (*22*). A summary of the source profiles used in this study is given in Table 2. The LDGV profile is characterized by high carbon content and a high OC/EC ratio (2.3). The HDDV profile is also characterized by high carbon content, but there the OC/EC ratio is much lower (0.27). The LDGV had a higher abundance of trace metals, compared to the HDDV profile. However, the relative amounts of EC and OC in emissions from both gasoline and diesel vehicles is highly variable, and there is significant overlap in the range of values between the two mobile source types (23). Therefore, trying to distinguish gasoline and diesel contributions separately on the basis of just EC and OC mass fractions is suspect (*23*). This further indicates the need for additional markers to accurately separate the emissions from each of these sources. The BURN profile is characterized by high carbon content and a high OC/EC ratio (4.1), but also by a high K content (0.057), which can serve as a marker for vegetative burning. Crustal elements, Al, Ca, Fe, and Si, along with OC, are abundant in the SDUST profile. The CFPP is characterized by high fractions of SO_4^{-2}, OC, Al, Ca, and Si, and by a relatively high Se content compared to other sources. Selenium can therefore serve as a marker for coal-fired power plants. Emissions from cement kilns are characterized by high fractions of SO_4^{-2}, NO_3^-, OC, Al, Ca, Fe, K, and Si. This shows that differentiating emissions from power plants, cement kilns, and fugitive soil dust might be subject to collinearity.

Adding information on gaseous emissions, in the form of gas-to-particle ratios, can further assist in identifying sources. Gas-to-particle ratios for mobile sources (LDGV, HDDV), based on the 1999 National Emissions Inventory (*14*), show very different patterns, with LDGV being characterized by a significantly higher $CO/PM_{2.5}$ ratio than HDDV (Table 3). Uncertainties in these ratios were not available, but are likely not large enough to mask the major differences between gaseous emissions from gasoline and diesel vehicles. Ratios for vegetative burning, coal-fired power plants, and cement kilns were determined on the basis of data from the BRAVO study (*19*) and the emission inventory for the State of Georgia (*24*). CO and NO_x ratios for cement kilns were modified to describe the kiln, rather than the entire plant emissions, as given by the inventory (which includes high particulate matter emissions from all grinding operations). The modification was based on the SO_2 ratio for kilns (*19*) compared to the SO_2 ratio obtained from the inventory. The high $SO_2/PM_{2.5}$ ratios in power plants and cement plants (Table 3) can assist in separating these emissions from fugitive soil dust (no gaseous emissions). The higher NO_x emissions from cement kilns, along with the differences in PM emissions, can assist in separating cement kilns and coal-fired power plant emissions. The relatively low $CO/PM_{2.5}$ ratios in vegetative burning emissions can serve as an additional marker to assist in separating this source from LDGV emissions (along with potassium).

Results

Source apportionment was performed on the SEARCH 25-month dataset using three different techniques. First, CMB8 (*1*, *2*) was used, applying effective variance weighting for

TABLE 2. Particulate Source Profiles Used in the Apportionment Process (Fraction of Total $PM_{2.5}$ Emissions and Standard Deviations over Multiple Measurements)

species	LDGV[a]	HDDV[a]	SDUST[b]	BURN[c]	CFPP[c]
SO_4^{-2}	0.0133 ± 0.0056	0.0046 ± 0.0048	0.0010 ± 0.0004	0.0239 ± 0.0227	0.2874 ± 0.2256
NO_3^-	0.0000 ± 0.0052	0.0020 ± 0.0014	0.0010 ± 0.0004	0.0024 ± 0.0018	0.0069 ± 0.0109
Cl-	0.0000 ± 0.0100	0.0011 ± 0.0003	0.0007 ± 0.0005	0.0761 ± 0.0730	0.0089 ± 0.0157
NH_4^+	0.0000 ± 0.0100	0.0000 ± 0.0100	0.0000 ± 0.0000	0.0165 ± 0.0253	0.0179 ± 0.0213
EC	0.2355 ± 0.0277	0.7351 ± 0.1014	0.0060 ± 0.0040	0.1575 ± 0.1545	0.0138 ± 0.0222
OC	0.5486 ± 0.0642	0.1981 ± 0.0774	0.0440 ± 0.0170	0.6441 ± 0.1645	0.2718 ± 0.2577
Al	0.0019 ± 0.0024	0.0000 ± 0.0100	0.0950 ± 0.0010	0.0011 ± 0.0010	0.0530 ± 0.0326
As	0.0000 ± 0.0006	0.0000 ± 0.0001	0.0000 ± 0.0000	0.0002 ± 0.0007	0.0000 ± 0.0006
Ba	0.0000 ± 0.0100	0.0000 ± 0.0100	0.0000 ± 0.0000	0.0000 ± 0.0003	0.0107 ± 0.0101
Br	0.0000 ± 0.0003	0.0000 ± 0.0000	0.0000 ± 0.0000	0.0008 ± 0.0009	0.0003 ± 0.0006
Ca	0.0118 ± 0.0016	0.0006 ± 0.0005	0.0180 ± 0.0040	0.0040 ± 0.0050	0.1655 ± 0.1053
Cu	0.0004 ± 0.0006	0.0000 ± 0.0001	0.0003 ± 0.0003	0.0000 ± 0.0000	0.0009 ± 0.0007
Fe	0.0120 ± 0.0016	0.0002 ± 0.0001	0.0530 ± 0.0060	0.0007 ± 0.0008	0.0361 ± 0.0202
K	0.0001 ± 0.0015	0.0001 ± 0.0002	0.0092 ± 0.0033	0.0573 ± 0.0563	0.0052 ± 0.0026
Mn	0.0001 ± 0.0008	0.0000 ± 0.0001	0.0016 ± 0.0007	0.0000 ± 0.0000	0.0012 ± 0.0011
Pb	0.0006 ± 0.0008	0.0000 ± 0.0001	0.0001 ± 0.0000	0.0000 ± 0.0000	0.0006 ± 0.0009
Sb	0.0000 ± 0.0100	0.0000 ± 0.0100	0.0000 ± 0.0000	0.0000 ± 0.0001	0.0001 ± 0.0005
Se	0.0000 ± 0.0003	0.0000 ± 0.0001	0.0000 ± 0.0000	0.0000 ± 0.0000	0.0058 ± 0.0083
Si	0.0121 ± 0.0193	0.0000 ± 0.0100	0.2660 ± 0.0140	0.0030 ± 0.0032	0.1069 ± 0.0681
Sn	0.0000 ± 0.0100	0.0000 ± 0.0100	0.0000 ± 0.0000	0.0000 ± 0.0001	0.0001 ± 0.0004
Ti	0.0001 ± 0.0067	0.0000 ± 0.0011	0.0100 ± 0.0010	0.0001 ± 0.0001	0.0085 ± 0.0052
Zn	0.0091 ± 0.0010	0.0006 ± 0.0003	0.0001 ± 0.0000	0.0003 ± 0.0002	0.0031 ± 0.0033

species	CEM[c]	AMSULF[d]	AMBSLF[d]	AMNITR[d]	OTHEROC[d]
SO_4^{-2}	0.3138 ± 0.0837	0.727 ± 0.036	0.835 ± 0.042	0.000 ± 0.000	0.00 ± 0.00
NO_3^-	0.0891 ± 0.0734	0.000 ± 0.000	0.000 ± 0.000	0.775 ± 0.039	0.00 ± 0.00
Cl^-	0.0712 ± 0.1255	0.000 ± 0.000	0.000 ± 0.000	0.000 ± 0.000	0.00 ± 0.00
NH_4^+	0.0236 ± 0.0187	0.273 ± 0.014	0.156 ± 0.008	0.225 ± 0.011	0.00 ± 0.00
EC	0.0296 ± 0.0250	0.000 ± 0.000	0.000 ± 0.000	0.000 ± 0.000	0.00 ± 0.00
OC	0.1278 ± 0.0603	0.000 ± 0.000	0.000 ± 0.000	0.000 ± 0.000	1.00 ± 0.00
Al	0.0106 ± 0.0035	0.000 ± 0.000	0.000 ± 0.000	0.000 ± 0.000	0.00 ± 0.00
As	0.0000 ± 0.0002	0.000 ± 0.000	0.000 ± 0.000	0.000 ± 0.000	0.00 ± 0.00
Ba	0.0004 ± 0.0012	0.000 ± 0.000	0.000 ± 0.000	0.000 ± 0.000	0.00 ± 0.00
Br	0.0011 ± 0.0013	0.000 ± 0.000	0.000 ± 0.000	0.000 ± 0.000	0.00 ± 0.00
Ca	0.1748 ± 0.0526	0.000 ± 0.000	0.000 ± 0.000	0.000 ± 0.000	0.00 ± 0.00
Cu	0.0002 ± 0.0001	0.000 ± 0.000	0.000 ± 0.000	0.000 ± 0.000	0.00 ± 0.00
Fe	0.0134 ± 0.0052	0.000 ± 0.000	0.000 ± 0.000	0.000 ± 0.000	0.00 ± 0.00
K	0.1159 ± 0.0618	0.000 ± 0.000	0.000 ± 0.000	0.000 ± 0.000	0.00 ± 0.00
Mn	0.0010 ± 0.0004	0.000 ± 0.000	0.000 ± 0.000	0.000 ± 0.000	0.00 ± 0.00
Pb	0.0006 ± 0.0008	0.000 ± 0.000	0.000 ± 0.000	0.000 ± 0.000	0.00 ± 0.00
Sb	0.0000 ± 0.0003	0.000 ± 0.000	0.000 ± 0.000	0.000 ± 0.000	0.00 ± 0.00
Se	0.0001 ± 0.0000	0.000 ± 0.000	0.000 ± 0.000	0.000 ± 0.000	0.00 ± 0.00
Si	0.0426 ± 0.0219	0.000 ± 0.000	0.000 ± 0.000	0.000 ± 0.000	0.00 ± 0.00
Sn	0.0001 ± 0.0002	0.000 ± 0.000	0.000 ± 0.000	0.000 ± 0.000	0.00 ± 0.00
Ti	0.0015 ± 0.0007	0.000 ± 0.000	0.000 ± 0.000	0.000 ± 0.000	0.00 ± 0.00
Zn	0.0041 ± 0.0059	0.000 ± 0.000	0.000 ± 0.000	0.000 ± 0.000	0.00 ± 0.00

[a] From the NFRAQS study (*21*). [b] From Cooper (*22*). [c] From Chow et al. (*19*). [d] Based on molecular-weight fractions.

least squares (EV) calculations (*3*) for $PM_{2.5}$ components only (i.e., gaseous species were not used as fitting species). Then, the uncertainties in the source profiles were set equal to zero, and CMB8 was run again, using the ordinary weighted least-squares (OWLS) solution (*3*) (once more, without using gaseous species in the weighting procedure). Finally, the Lipschitz(−continuous) global optimizer (LGO) (*15*, *16*) was applied to perform the OWLS solution, forcing constraints on the calculated levels of SO_2, CO, and NO_x. An LGO-derived OWLS solution without forcing gas-phase constraints was similar to the CMB OWLS solution. Applying an EV solution to LGO and forcing gas-phase constraints turned out to be too irregular, due to the rigidity of the EV weighting function. The measures used to evaluate each individual solution achieved were the chi-square (eq 2), the correlation coefficient, the fraction of total $PM_{2.5}$ mass apportioned, and the calculated-to-observed ratios for the individual ratios. However, the chi-square values from EV are not comparable with the ones achieved by OWLS, since the denominator in its formula is different. Therefore, as a convenient uniform measure of the quality of the fit, we also calculated daily values for the normalized mean-square-error (NMSE), given as

$$\mathrm{NMSE} = \frac{\sum_{i=1}^{m}(C_i - \sum_{j=1}^{n} f_{i,j}S_j)^2}{\sum_{i=1}^{m}(C_i \sum_{j=1}^{n} f_{i,j}S_j)} \qquad (4)$$

The NMSE has a range of $0 \le \mathrm{NMSE} \le \infty$, with 0 meaning perfect agreement in value between modeled and ambient values. A NMSE value of 0.5 represents a factor of 2, on the average, between the two sets of data.

The average source-contributions, based on the entire 25-month dataset (average of 762 daily values) and using these three techniques, indicate that a major part of the ambient $PM_{2.5}$ is of secondary origin (Figure 1; Table 4. The apportionment of the primary pollutants differed among the

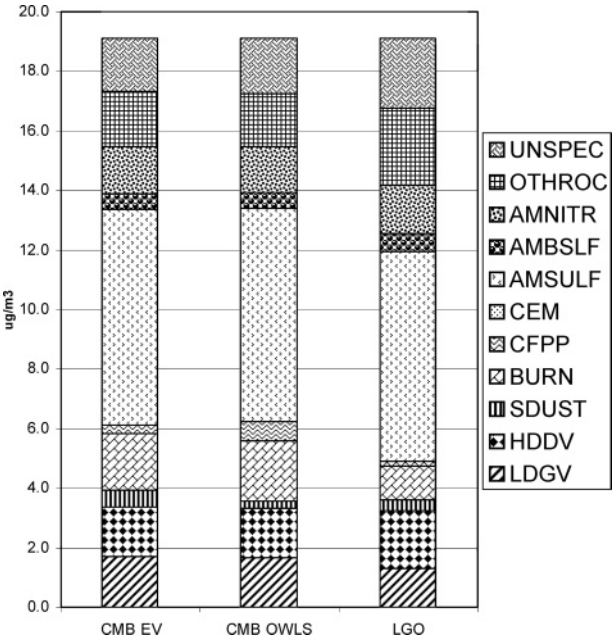

FIGURE 1. Source-contributions to $PM_{2.5}$ levels at JST site, Atlanta, GA, using CMB8 EV solution, CMB8 OWLS solution, and LGO.

TABLE 3. Gas-to-$PM_{2.5}$ Ratios Used as Constraints in the Optimization Process (Mass/Mass)

source	$SO_2/PM_{2.5}$	$CO/PM_{2.5}$	$NO_x/PM_{2.5}$
LDGV	4.0[a]	800[a]	83.7[a]
HDDV	0.71[a]	13.4[a]	21.9[a]
BURN	0.013 ± 0.0004[b]	10.1 ± 1.1[b]	0.24 ± 0.06[b]
CFPP	128 ± 29.4[c]	2.1 ± 0.7[c]	41.0 ± 14.5[c]
CEM	316 ± 210[c,d]	5.3 ± 6.5[c,d]	270 ± 344[c,d]

[a] Based on emission inventory data, no variability provided. [b] Based on emission inventory data; standard deviations based on county level, therefore low. [c] Based on emission inventory data; standard deviations based on plant level, therefore higher. [d] Based on source-profile measurements (*19*).

three techniques used. The CMB8 EV solution apportioned 3.4 $\mu g/m^3$ to mobile sources, with a diesel-to-gasoline ratio of 0.97. A slightly lower contribution was apportioned to mobile sources using the OWLS solution (3.3 $\mu g/m^3$), with a similar diesel-to-gasoline ratio. The LGO based mobile source contribution was slightly lower (3.2 $\mu g/m^3$), with a higher diesel-to-gasoline ratio (1.53). This lower gasoline vehicle contribution is also evident in the lower calculated-to-observed ratio for CO based on the LGO solution, compared to the EV and OWLS solutions (all over-predicted). Another notable difference between the three solutions was the amount of $PM_{2.5}$ attributed to power plants. CMB8-EV estimated that contribution at 0.29 $\mu g/m^3$, CMB−OWLS estimated it at 0.62 $\mu g/m^3$, and LGO estimated the contribution at 0.15 $\mu g/m^3$. These differences are also evident in the calculated-to-observed ratios for SO_2, which are significantly overpredicted in the EV and OWLS solutions. The amount attributed to vegetative burning was fairly similar in the EV and OWLS solutions (1.9 and 2.0 $\mu g/m^3$, respectively), significantly higher than that in the LGO solution (1.1 $\mu g/m^3$). Potassium, a marker for vegetative burning, is overpredicted in the EV and OWLS solutions (calculated-to-observed ratios of 2.2), and better predicted in the LGO solution (ratio of 1.2). Differences were also noticed in the fugitive soil dust contributions. The amount attributed to the "Other OC" category was lower in the two CMB applications compared to the LGO solution, most likely due to overestimation of the OC contribution from gasoline vehicles and vegetative burning.

It is interesting to note that all three solutions are characterized by high correlation coefficients for the fit obtained (0.97−0.99), good mass closure (91−93%), and calculated-to-observed ratios nearing one for the major $PM_{2.5}$ components. In the EV solution, the average chi-square value, and most individual values, lied within the acceptable range (<4) (*1*, *2*). The chi-square values based on the OWLS and LGO solutions are not comparable to that of the EV solution. The chi-square based on the LGO solution is significantly higher than that in the OWLS solution, and reflects the "penalty" of bounding acceptable solutions based on the gas-phase species. However, the correlation coefficient is higher, and the overall and trace-metal-based NMSE values are lower for the LGO solution compared to the OWLS solution.

To address the sensitivity of the solution obtained to the factor used as a constraint for the gas-phase species, we also conducted the same analysis using a factor of 2 (instead of three). Results obtained were nearly identical, with mass contributions differing by less than 7% for most sources. The major difference observed was for the average LDGV contribution, 0.2 $\mu g/m^3$ (18%). The source cross correlations between these two sets of solution were higher than 0.92 for all sources except cement kilns ($R = 0.62$, but mass contribution being extremely low).

To analyze the driving forces in the apportionment process, we calculated the correlations between the daily contributions of the various sources and the daily ambient levels of the different species. These correlations (R values, Table 5) indicate which are the species most highly correlated with each source category, therefore driving the apportionment. This is done on the entire dataset, as opposed to the transpose of the normalized modified pseudo-inverse matrix (MPIN) (*2*), which indicates the degree of influence each species concentration has on the contribution, on a case by case basis. Note that the correlations used here are not normalized, hence the species with the highest correlations are considered the ones most influential, even if the actual correlation is somewhat low. The following is stated based on these correlations.

LDGV. The LDGV contribution based on the CMB-EV solution is correlated mainly with Zn, OC, and EC. A low correlation with CO and NO_y is observed in the EV solution. The OWLS solution showed a fairly similar pattern, with slightly higher correlations with CO and NO_y, and a fairly high correlation with Pb. However, the LGO solution was highly correlated with CO and NO_y, along with much of the same PM species as the EV and OWLS solutions.

HDDV. The HDDV contribution generated by all three source-apportionment techniques used here was most correlated with EC, which is the major component of diesel emissions. Stronger correlations with EC were observed in the OWLS and LGO solutions. Correlation with NO_y was the highest in the LGO solution. Such a correlation is expected because NO_x emissions from diesel vehicles, on a per-mile basis, are higher than those from gasoline vehicles (*25*, *26*).

BURN. The vegetative burning contribution from the EV and OWLS solution was correlated with chlorine, potassium, EC, OC, and bromine. The LGO solution was correlated with the same species except bromine. The correlation with potassium was much higher in the LGO solution (0.62) compared to that with the EV and OWLS solutions (0.37 and 0.43, respectively).

SDUST. Soil dust is characterized by a high abundance of crustal elements, such as Al, Ca, Fe, Si, and Ti. Results from the all three solutions are correlated with these elements. However, the EV solution is most correlated with Fe, and to a degree with Si, Ti, and Mn, while the OWLS and LGO solutions are correlated mainly with Si, Al, Ti, and Fe. As

TABLE 4. Average and Standard Deviation of the Source-Contributions to $PM_{2.5}$ Levels Measured at JST Site, Atlanta, GA, Using CMB8-EV, CMB8-OWLS, and LGO (Also Reported Are the Correlation (*R*), NMSE, % Total Mass, Chi-square and Calculated-to-Observed Ratios)

	mean (SD)		
	CMB8-EV	**CMB8-OWLS**	**LGO**
R^a	0.9734 (0.0298)	0.9661 (0.0357)	0.9879 (0.0324)
NMSE $PM_{2.5}$[a]	0.161 (0.362)	0.0327 (0.131)	0.026 (0.096)
NMSE metals[b]	0.801 (0.966)	0.714 (0.901)	0.249 (0.346)
% total mass[c]	93.4 (18.2)	93.1 (18.7)	90.5 (17.4)
Chi-square[d]	3.16 (3.47)	4.48 (6.45)	20.3 (16.8)
LDGV ($\mu g/m^3$)	1.72 (1.61)	1.68 (1.55)	1.28 (0.90)
HDDV ($\mu g/m^3$)	1.66 (1.53)	1.62 (1.52)	1.96 (1.63)
SDUST ($\mu g/m^3$)	0.55 (0.61)	0.28 (0.45)	0.39 (0.48)
BURN ($\mu g/m^3$)	1.90 (1.29)	2.01 (1.50)	1.13 (0.69)
CFPP ($\mu g/m^3$)	0.29 (0.48)	0.62 (0.74)	0.15 (0.12)
CEM ($\mu g/m^3$)	0.006 (0.04)	0.012 (0.08)	0.004 (0.02)
AMSULF ($\mu g/m^3$)	7.23 (5.20)	7.19 (5.17)	7.03 (5.12)
AMBSLF ($\mu g/m^3$)	0.54 (1.30)	0.50 (1.28)	0.64 (1.46)
AMNITR ($\mu g/m^3$)	1.57 (1.25)	1.55 (1.25)	1.60 (1.34)
OTHEROC ($\mu g/m^3$)	1.86 (1.55)	1.76 (1.50)	2.59 (1.64)
SO_4^{-2} ratio[e]	1.16 (0.47)	1.10 (0.12)	1.07 (0.07)
NO_3^- ratio[e]	1.25 (1.02)	1.14 (0.75)	1.18 (0.87)
Cl^- ratio[e]	1.81 (1.49)	1.85 (1.36)	1.06 (0.63)
NH_4^+ ratio[e]	0.93 (0.38)	0.89 (0.14)	0.88 (0.15)
EC ratio[e]	1.09 (0.78)	0.97 (0.14)	0.98 (0.13)
OC ratio[e]	1.06 (0.51)	1.01 (0.19)	1.00 (0.03)
Al ratio[e,f]	7.82 (6.37)	6.64 (5.11)	4.67 (2.81)
As ratio[e]	0.53 (0.47)	0.55 (0.51)	0.32 (0.25)
Ba ratio[e]	0.18 (0.28)	0.38 (0.45)	0.10 (0.08)
Br ratio[e]	0.68 (0.92)	0.68 (0.84)	0.39 (0.38)
Ca ratio[e]	1.87 (1.48)	2.92 (2.60)	1.15 (0.34)
Cu ratio[e]	0.59 (0.57)	0.60 (0.52)	0.42 (0.39)
Fe ratio[e]	0.84 (0.66)	0.73 (0.38)	0.55 (0.17)
K ratio[e]	2.23 (1.72)	2.20 (1.55)	1.19 (0.49)
Mn ratio[e]	1.06 (1.08)	0.94 (0.88)	0.69 (0.58)
Pb ratio[e]	0.37 (0.38)	0.36 (0.36)	0.27 (0.23)
Sb ratio[e]	0.02 (0.02)	0.03 (0.03)	0.01 (0.01)
Se ratio[e]	1.99 (4.05)	4.66 (7.72)	1.11 (1.20)
Si ratio[e]	2.18 (1.54)	1.64 (0.77)	1.28 (0.12)
Sn ratio[e]	0.02 (0.02)	0.02 (0.02)	0.01 (0.00)
Ti ratio[e]	2.12 (1.59)	2.01 (1.57)	1.27 (0.70)
Zn ratio[e]	1.42 (1.95)	1.22 (0.73)	1.01 (0.35)
SO_2 ratio[e,f]	4.37 (8.73)	8.24 (23.4)	1.99 (0.97)
CO ratio[e,f]	3.18 (3.43)	3.07 (3.56)	2.06 (0.83)
NO_y ratio[e,f]	2.11 (1.83)	2.07 (1.51)	1.58 (0.66)

[a] Calculated based on all $PM_{2.5}$ components. [b] Calculated based on trace metals only. [c] % of apportioned mass to total $PM_{2.5}$. [d] Chi-square is not comparable for the EV case and the two OWLS cases, as the denominator in its formula is different. [e] Ratio of apportioned mass to ambient level (ideally would approach 1 for all species). [f] Not used as a fitting species.

expected, low correlations with the gaseous species were found. However, the EV solution seems to have picked a contribution associated with motor vehicles (possibly re-suspended paved road dust), as it is somewhat correlated with EC and CO, as opposed to the OWLS and LGO solutions.

CFPP. The EV-generated power plant contribution is mostly correlated with Cu, SO_4^{-2}, Ca, and to a degree with Se and Fe. The OWLS solution is mostly correlated with Cu, Fe, and Mn. Both these solutions show no correlation with SO_2, and the OWLS solution shows a correlation with CO and NO_y, indicative of mobile sources. The LGO solution, however, is mostly correlated with Ca, Se, and SO_2. Se is a unique marker for coal-fired power plant emissions (*2*). The LGO solution, being correlated with both Se and SO_2, is likely truly indicative of power plants.

CEM. It is difficult to evaluate the driving species for the cement kiln contribution, as it is very low. Nonzero contributions were generated in only 33, 36, and 65 cases (out of 762 cases), using EV, OWLS, and LGO, respectively. On the basis of these limited data, the EV solution was mainly correlated with Ca; the OWLS solution was correlated with Br; and the LGO solution was correlated with Ca and the NO_x.

OTHEROC. The other OC category includes any OC not apportioned to one of the previous categories. If most of the primary OC was accounted for, this category would include mainly secondary OC. Since EC and OC often share the same sources (*25*), a high correlation of the OTHEROC category with either EC or OC would indicate a primary OC contribution. A good reference point is the correlation between OC and EC in the ambient data, which is 0.82. The correlations between EC and the contributions to the OTHEROC category are lower: 0.44, 0.60, and 0.65 for the EV, OWLS, and LGO solutions, respectively. This indicates a secondary component in the OTHEROC category. These values, along with the correlations with OC and the magnitude of the contribution, suggest that LGO solution includes more primary OC than the EV and OWLS solutions. This is likely due to an over estimation of the mobile-source contribution by both EV and OWLS, leaving less OC to be apportioned to the OTHEROC category. This does mean, however, that there is an unexplained source of OC in the LGO solution. One likely source would be meat charbroiling, which, as previously mentioned, emits almost solely OC, and is characterized by low gas-to-particle ratios. For this reason, it is difficult to distinguish meat charbroiling from secondary OC formation

TABLE 5. Correlations (*R*) between Source Contributions and Ambient Levels of Fitting Species

	CMB-EV	CMB-OWLS	LGO	CMB-EV	CMB-OWLS	LGO	CMB-EV	CMB-OWLS	LGO	CMB-EV	CMB-OWLS	LGO
	LDGV			HDDV			BURN			SDUST		
SO_4^{-2}	0.03	0.01	0.04	0.22	0.22	0.21	0.10	0.07	0.14	0.20	0.17	0.24
NO_3^-	0.22	0.31	0.30	0.14	0.18	0.19	0.15	0.23	0.33	0.01	−0.09	−0.09
Cl^-	0.16	0.17	0.09	0.05	0.04	0.11	0.35	0.45	0.52	0.02	−0.01	−0.01
NH_4^+	0.08	0.05	0.04	0.27	0.25	0.26	0.22	0.23	0.18	0.29	0.21	0.28
EC	0.42	0.53	0.39	0.69	0.94	0.96	0.34	0.43	0.41	0.40	0.21	0.25
OC	0.45	0.55	0.45	0.53	0.68	0.74	0.35	0.49	0.49	0.33	0.13	0.19
Al	0.00	0.04	0.07	0.05	0.09	0.08	0.03	0.04	0.13	0.29	0.91	0.87
As	0.26	0.32	0.27	0.21	0.23	0.29	0.30	0.42	0.29	0.16	0.05	0.05
Ba	−0.01	0.01	0.03	0.09	0.13	0.10	0.04	0.05	0.10	0.11	0.21	0.22
Br	0.13	0.15	0.13	0.35	0.34	0.17	0.38	0.41	0.14	0.24	0.04	0.01
Ca	0.24	0.30	0.39	0.25	0.34	0.32	0.17	0.19	0.19	0.33	0.62	0.57
Cu	0.38	0.50	0.36	0.25	0.30	0.38	0.22	0.38	0.29	0.37	0.31	0.24
Fe	0.36	0.46	0.40	0.45	0.56	0.60	0.24	0.34	0.33	0.57	0.76	0.77
K	0.23	0.27	0.22	0.24	0.30	0.35	0.37	0.43	0.62	0.30	0.42	0.29
Mn	0.41	0.51	0.36	0.41	0.53	0.58	0.24	0.34	0.32	0.46	0.53	0.53
Pb	0.42	0.65	0.34	0.19	0.22	0.33	0.18	0.32	0.33	0.24	0.07	0.06
Sb	0.06	0.06	0.06	0.06	0.11	0.07	0.25	0.26	0.00	0.05	0.00	−0.01
Se	0.13	0.17	0.13	0.34	0.38	0.41	0.23	0.27	0.17	0.15	0.12	0.15
Si	0.12	0.17	0.20	0.22	0.27	0.27	0.12	0.16	0.22	0.48	0.95	0.99
Sn	0.16	0.21	0.16	0.13	0.14	0.14	0.08	0.13	0.11	0.08	0.06	0.12
Ti	0.14	0.18	0.18	0.27	0.35	0.37	0.19	0.25	0.29	0.44	0.83	0.84
Zn	0.58	0.86	0.46	0.31	0.38	0.42	0.20	0.37	0.33	0.29	0.08	0.12
SO_2	0.18	0.23	0.25	0.21	0.31	0.33	0.17	0.20	0.20	0.09	−0.03	−0.03
CO	0.31	0.36	0.74	0.23	0.37	0.32	0.15	0.25	0.24	0.23	0.11	0.14
NO_y	0.31	0.40	0.66	0.28	0.42	0.45	0.19	0.29	0.25	0.20	0.04	0.07

	CMB-EV	CMB-OWLS	LGO	CMB-EV	CMB-OWLS	LGO	CMB-EV	CMB-OWLS	LGO
	CFPP			CEM			AMSULF		
SO_4^{-2}	0.43	0.28	0.28	−0.11	0.15	0.02	0.85	0.94	0.93
NO_3^-	0.07	0.17	0.14	0.29	0.37	0.04	−0.06	−0.01	−0.01
Cl^-	0.01	0.10	0.08	−0.08	0.15	−0.18	0.04	0.07	0.07
NH_4^+	0.43	0.33	0.24	−0.12	0.10	−0.06	0.85	0.95	0.94
EC	0.34	0.54	0.42	−0.15	0.06	0.13	0.16	0.22	0.22
OC	0.27	0.48	0.38	−0.13	0.17	0.17	0.22	0.28	0.28
Al	0.03	0.13	0.09	0.09	−0.09	−0.13	0.00	0.03	0.03
As	0.07	0.23	0.18	0.24	0.46	0.23	−0.02	0.00	0.00
Ba	0.23	0.25	0.12	−0.04	−0.08	0.12	0.14	0.18	0.18
Br	0.10	0.16	0.12	0.01	0.58	0.11	−0.02	0.01	0.01
Ca	0.43	0.46	0.56	0.44	0.37	0.56	0.24	0.30	0.30
Cu	0.46	0.74	0.21	0.24	0.14	−0.03	0.07	0.10	0.10
Fe	0.36	0.62	0.40	0.18	0.28	0.05	0.20	0.27	0.27
K	0.17	0.34	0.17	−0.15	0.05	−0.05	0.12	0.15	0.15
Mn	0.33	0.61	0.33	0.18	0.23	−0.05	0.17	0.23	0.23
Pb	0.13	0.49	0.11	−0.07	0.18	0.16	−0.05	−0.03	−0.02
Sb	0.08	0.13	0.08	−0.28	0.04	0.11	−0.06	−0.05	−0.04
Se	0.36	0.29	0.50	0.12	−0.01	0.24	0.32	0.37	0.37
Si	0.22	0.34	0.28	0.22	0.07	0.02	0.23	0.28	0.28
Sn	0.02	0.21	0.05	−0.07	0.12	0.15	0.01	0.03	0.03
Ti	0.27	0.43	0.27	0.05	0.06	−0.13	0.25	0.31	0.30
Zn	0.14	0.50	0.27	0.29	0.24	0.25	0.01	0.04	0.05
SO_2	0.11	0.21	0.45	0.18	−0.12	0.25	−0.12	−0.08	−0.08
CO	0.17	0.43	0.19	0.11	0.06	0.18	−0.03	0.00	0.00
NO_y	0.16	0.41	0.31	0.14	0.11	0.40	−0.10	−0.07	−0.07

using either CMB (without organic markers) or this application of LGO. An organic marker, such as cholesterol, is needed to identify and quantify meat charbroiling emissions.

AMSULF, AMBSLF, AMNITR. These secondary "sources" were all correlated with their major components, and low correlations with gaseous pollutants were observed, for all three cases.

To further illustrate the differences between the EV, OWLS, and LGO solutions, we also calculated source intercorrelations using these three solutions (Table 6). The diagonal terms in these matrixes indicate that the contributions of ammonium sulfate, ammonium bisulfate, and ammonium nitrate are fairly similar in all three cases. However, major differences are observed for the primary source categories. The EV and OWLS gasoline vehicle contribution is significantly different than the LGO LDGV contribution, as shown by the low correlations. The differences in the HDDV contributions are more subtle. Another major difference is observed in the CFPP contribution: the OWLS CFPP contribution is correlated more with the LDGV contribution from LGO than the corresponding CFPP contributions, likely due to collinearity.

Results from the LGO solution (based on inorganic markers and inorganic gases) were also compared with results from an organic markers source-apportionment study (*4*) and the five-county Atlanta metropolitan area emissions inventory (*24*) (Table 7). In the Zheng et al. study (*4*), average monthly contributions to $PM_{2.5}$ were calculated for the

TABLE 5. Continued

	CMB-EV	CMB-OWLS	LGO	CMB-EV	CMB-OWLS	LGO	CMB-EV	CMB-OWLS	LGO
	AMBSULF			AMNITR			OTHER OC		
SO_4^{-2}	0.46	0.52	0.54	0.04	0.05	0.06	0.22	0.23	0.29
NO_3^-	−0.01	0.04	0.05	0.68	0.87	0.82	0.08	0.08	0.14
Cl^-	−0.05	0.03	0.05	0.22	0.30	0.26	0.05	−0.01	0.08
NH_4^+	0.29	0.36	0.40	0.08	0.11	0.11	0.25	0.23	0.29
EC	−0.07	0.03	0.00	0.17	0.22	0.21	0.44	0.60	0.65
OC	0.01	0.09	0.06	0.20	0.23	0.23	0.63	0.81	0.92
Al	0.09	0.15	0.09	−0.04	−0.03	−0.04	−0.03	0.00	−0.04
As	−0.06	−0.01	−0.02	0.10	0.14	0.14	0.12	0.15	0.27
Ba	0.09	0.06	0.01	0.01	0.02	0.02	0.06	0.12	0.10
Br	0.00	0.07	0.09	0.08	0.09	0.09	0.29	0.30	0.14
Ca	0.07	0.16	0.17	0.04	0.06	0.05	0.15	0.20	0.21
Cu	−0.02	0.06	−0.02	0.08	0.12	0.11	0.30	0.28	0.32
Fe	0.04	0.14	0.08	0.07	0.12	0.10	0.32	0.36	0.37
K	0.04	0.09	0.04	0.09	0.10	0.11	0.33	0.45	0.36
Mn	0.01	0.07	0.02	0.13	0.18	0.16	0.24	0.23	0.34
Pb	−0.05	0.05	−0.04	0.14	0.22	0.20	0.25	0.25	0.35
Sb	−0.07	0.02	−0.01	−0.01	0.01	0.01	0.03	0.07	0.07
Se	0.14	0.18	0.23	0.12	0.12	0.12	0.09	0.12	0.24
Si	0.22	0.25	0.23	−0.04	−0.04	−0.05	0.15	0.21	0.16
Sn	0.07	0.09	0.03	0.10	0.08	0.07	0.09	0.11	0.12
Ti	0.11	0.28	0.22	−0.03	−0.01	−0.01	0.17	0.23	0.21
Zn	−0.07	−0.03	−0.06	0.16	0.19	0.17	0.27	0.24	0.39
SO_2	−0.08	0.00	−0.02	0.16	0.18	0.18	0.08	0.12	0.24
CO	−0.05	−0.02	−0.01	0.13	0.15	0.16	0.24	0.27	0.24
NO_y	−0.09	−0.05	−0.06	0.18	0.22	0.21	0.19	0.26	0.29

TABLE 6. Source Intercorrelations (*R*) Using CMB8-EV, CMB8-OWLS, and LGO

		LDGV	HDDV	SDUST	BURN	CFPP	CEM	AMSULF	AMBSLF	AMNITR	OTHROC
		EV									
OWLS	LDGV	**0.64**	0.30	0.31	0.22	0.14	0.23	−0.03	−0.05	0.19	0.25
	HDDV	0.26	**0.69**	0.33	0.21	0.34	−0.20	0.16	−0.10	0.12	0.39
	SDUST	0.00	0.13	**0.42**	0.08	0.15	−0.10	0.16	0.25	−0.08	0.07
	BURN	0.37	0.26	0.28	**0.69**	0.17	−0.08	0.07	−0.06	0.15	0.21
	CFPP	0.41	0.40	0.41	0.28	**0.65**	0.15	0.25	−0.09	0.13	0.24
	CEM	0.29	0.24	0.32	0.21	0.00	**0.81**	0.11	0.25	0.31	0.61
	AMSULF	0.04	0.25	0.26	0.15	0.46	−0.14	**0.90**	0.19	−0.01	0.22
	AMBSLF	−0.03	0.00	0.16	−0.05	0.02	0.13	0.22	**0.91**	0.01	0.10
	AMNITR	0.18	0.12	0.01	0.11	0.06	0.18	−0.04	0.01	**0.77**	0.10
	OTHROC	0.16	0.44	0.16	0.15	0.17	−0.29	0.17	0.05	0.08	**0.68**
		LGO									
EV	LDGV	**0.44**	0.36	0.07	0.30	0.16	0.15	0.04	−0.02	0.16	0.32
	HDDV	0.17	**0.74**	0.19	0.28	0.31	0.19	0.25	0.00	0.11	0.45
	SDUST	0.23	0.38	**0.47**	0.23	0.16	−0.03	0.26	0.08	0.00	0.23
	BURN	0.16	0.32	0.10	**0.46**	0.16	0.07	0.14	0.04	0.11	0.24
	CFPP	0.14	0.33	0.20	0.13	**0.37**	0.31	0.46	0.02	0.06	0.21
	CEM	0.18	−0.23	0.20	−0.06	0.25	**1.00**	−0.14	0.22	0.16	−0.23
	AMSULF	−0.01	0.16	0.23	0.07	0.21	−0.05	**0.89**	0.27	−0.03	0.22
	AMBSLF	−0.03	−0.09	0.22	0.00	0.02	0.24	0.18	**0.86**	0.00	0.04
	AMNITR	0.20	0.12	−0.07	0.24	0.06	−0.05	−0.01	0.05	**0.76**	0.13
	OTHROC	0.18	0.43	0.13	0.26	0.17	0.35	0.21	0.09	0.09	**0.66**
		LGO									
OWLS	LDGV	**0.54**	0.45	0.11	0.33	0.25	0.20	0.01	−0.03	0.24	0.40
	HDDV	0.24	**0.93**	0.23	0.29	0.40	0.13	0.23	0.01	0.17	0.58
	SDUST	0.08	0.18	**0.96**	0.16	0.16	−0.02	0.20	0.19	−0.08	0.06
	BURN	0.26	0.40	0.13	**0.59**	0.16	0.12	0.12	0.02	0.16	0.34
	CFPP	0.43	0.51	0.31	0.31	**0.37**	0.00	0.32	−0.08	0.17	0.33
	CEM	0.06	0.11	0.09	0.29	0.13	**0.30**	0.11	0.45	0.35	0.08
	AMSULF	0.02	0.23	0.28	0.13	0.26	−0.02	**0.99**	0.27	0.00	0.28
	AMBSLF	−0.02	0.02	0.24	0.09	0.13	0.51	0.20	**0.95**	0.05	0.14
	AMNITR	0.25	0.19	−0.07	0.27	0.10	0.03	−0.02	0.09	**0.97**	0.16
	OTHROC	0.18	0.58	0.18	0.24	0.21	0.31	0.20	0.08	0.12	**0.88**

months of April, July, August, and October of 1999, and January 2002, for the JST site, and are averaged here. Source categories included were diesel exhaust, gasoline exhaust, vegetative detritus, meat cooking, road dust, wood combustion, and natural gas combustion. Both the LGO solution and the Zheng et al. (*4*) results indicate the dominance of contributions from mobile sources to primary $PM_{2.5}$ levels, but the magnitude is somewhat different (66% and 58%, respectively). The split between gasoline and diesel vehicles also was different: a diesel-to-gasoline ratio of 1.5 using LGO and 6.7 using organic tracers. For comparison, the diesel-to-gasoline ratio in the emissions inventory for the five-county

TABLE 7. Comparison between Percent Contributions to Primary $PM_{2.5}$ Levels Based on LGO, Organic Marker CMB (*4*), and the Five-county Atlanta Metropolitan Area Emissions Inventory (*24*)[a]

source category (% contribution)	LGO	CMB using organic tracers (4)	5-county Atlanta metro emissions inventory (with/without "other" sources)
gasoline engines	26.0	7.5	3.9/7.6
diesel engines	39.9	50.3	11.5/22
fugitive soil dust	7.9	2.5	15.1/29[f]
vegetative burning/ wood combustion	23.0	29.7	15.1/29
coal-fired power plants	3.1		0.8/1.5
cement kilns	0.1		0.3/0.4
meat charbroiling		6.4	5.0/9.7[e]
vegetative detritus		2.7	
natural gas combustion		1.0	
other area sources[b]			43.9
other point sources[c]			2.7
other nonroad sources[d]			1.8

[a] The Zheng et al. results (4) were averaged to represent a yearly pattern by weighting July and August results as "summer", October as "fall", January as "winter" and April as "spring". Cooking emissions reported here are based on a preliminary estimate (27), and are not reported in the inventory (24). Inventoried emissions are given with and without "other" sources for more direct comparison. [b] Other than soil dust and wood combustion. [c] Other than coal-fired power plants and cement kilns. [d] Other than gasoline and diesel engines. [e] Based on a preliminary estimate by Baek et al. (*27*). [f] A large fraction of the fugitive dust emissions are expected to be removed locally.

Atlanta metropolitan area is 3.0 (22). Other differences were the somewhat lower vegetative burning contribution using LGO compared to organic markers (23% and 30%), the higher LGO soil dust contribution (7.9% compared to 2.5%), and the meat charbroiling contribution identified by the organic markers study (6.4%). The LGO solution generated a higher "secondary/other OC" contribution compared to the organic marker study (not presented in Table 7), which may include meat cooking emissions (characterized almost solely by OC emissions). In contrast to the receptor model results, the emissions inventory is dominated by area sources other than soil dust and wood combustion (44% of total $PM_{2.5}$ emissions). Wood combustion and road dust are the next two major sources in the inventory (15% each), followed by diesel and gasoline engines (11.5% and 3.9%, respectively). The road dust emissions seem to be over estimated, as shown by the receptor model results and measured levels of crustal species. Incorporating preliminary data on emissions from meat charbroiling (*27*) into the inventory suggests these emissions contribute 5% of total $PM_{2.5}$ emissions (not formally reported in the inventory, *24*). Given the dominance of "other" area sources (waste disposal treatment, recovery, and incineration; industrial oil and gas production; agriculture production; other sources) in the emissions inventory, it is difficult to compare the inventory to the source apportionment results directly. It seems that the "other" area source category is over-estimated, as four different sets of source apportionment results presented here (CMB EV, CMB OWLS, LGO, and the Zheng et al. study from 2002) indicate the dominance of contributions from diesel and gasoline engines to primary $PM_{2.5}$ levels (58−66% of $PM_{2.5}$ emissions, compared to 15% in the inventory). The contributions of coal-fired power plants and cement kilns, as indicated by the inventory, are relatively small, similar to findings from the LGO solution.

Acknowledgments

This work was supported by grants to Emory University from the U.S. Environmental Protection Agency (R82921301-0) and the National Institute of Environmental Health Sciences (R01ES11199 and R01ES11294) and to Georgia Tech (EPA grants R831076 and R830960). We also thank Georgia Power and Southern Company for continuing support and the individuals at ARA (Atmospheric Research and Analysis) for both providing access to data used in this analysis and ongoing discussions.

Literature Cited

(1) U.S.EPA. *CMB8 User's Manual*; EPA-454/R-01-XXX; Office of Air Quality, Planning and Standards: Research Triangle Park, NC, 2001.
(2) U.S.EPA. *CMB8 Application and Validation Protocol for $PM_{2.5}$ and VOC*; EPA-454/R-98-XXX; Office of Air Quality, Planning and Standards: Research Triangle Park, NC, 1998.
(3) Watson, J. G.; Cooper, J. A.; Huntzicker, J. J. The effective variance weighting for least squares calculations applied to the mass balance receptor model. *Atmos. Environ.* **1984**, *18*, 1347−1355.
(4) Zheng, M.; Cass, G. R.; Schauer, J. J.; Edgerton, E. S. Source apportionment of $PM_{2.5}$ in the southeastern United States using solvent-extractable organic compounds as tracers. *Environ. Sci. Technol.* **2002**, *36*, 2361−2371.
(5) Schauer, J. J.; Kleeman, M. J.; Cass, G. R.; Simoneit, A. T. Measurement of emissions from air pollution sources. 3. C_1−C_{29} organic compounds from fireplace combustion of wood. *Environ. Sci. Technol.* **2001**, *35*, 1716−1728.
(6) Schauer, J. J.; Kleeman, M. J.; Cass, G. R.; Simoneit, A. T. Measurement of emissions from air pollution sources. 2. C_1 through C_{30} organic compounds from medium duty diesel trucks. *Environ. Sci. Technol.* **1999**, *33*, 1578−1587.
(7) Seinfeld, J. H.; Pandis, S. N. *Atmospheric Chemistry and Physics*; John Wiley & Sons: New York, 1998.
(8) Wilson, W. E.; Suh, H. H. Fine particles and coarse particles: Concentration relationships relevant to epidemiologic studies. *J. Air Waste Manage. Assoc.* **1997**, *47*, 1238−1249.
(9) Lin, J.; Scheff, P. A.; Wadden, R. A. *Development of a Two-Phase Receptor Model for NMHC and PM_{10} Air Pollution Sources in Chicago*. Presented at the 86th Annual Meeting & exhibition of the Air & Waste Management Association: Denver, CO, 1993.
(10) Wadden, R. A.; Scheff, P. A.; Lin. J.; Lee, H.; Keil, C.; Graf-Teterycz, J.; Keehan, K.; Kenski, D.; Milz, S.; Holsen, T. M.; Khalili, N. *Two Phase Receptor Modeling*. Presented at the 84th Annual Meeting & Exhibition of the Air & Waste Management Association: Vancouver, BC, 1991.
(11) McKee, G. A.; Wadden, R. A.; and Scheff, P. A. *Development of a Two-Phase Chemical Mass Balance Receptor Model*. Presented at the 83rd Annual Meeting & Exhibition of the Air & Waste Management Association: Pittsburgh, PA, 1990.
(12) Scheff, P. A.; Wadden, R. A.; Allen, R. J. Development and Validation of a Chemical Element Mass Balance for Chicago. *Environ. Sci. Technol.* **1984**, *18*, 923−931.
(13) Lin, C.; Milford, J. B. Decay-adjusted chemical mass balance receptor modeling for volatile organic compounds. *Atmos. Environ.* **1994**, *28*, 3261−3276.
(14) U.S.EPA. 1999 National Emission Inventory (NEI): Air Pollutant Emission Trend (www.epa.gov/ttn/chief/trends/).
(15) Pinter, J. D. *Global Optimization in Action*; Kluwer Academic Publishers: Dordrecht, The Netherlands, 1996.
(16) Pintér, J. D. LGO—A Program System for Continuous and Lipschitz Global Optimization. In *Developments in Global Optimization*; Bomze, I. M., Csendes, T., Horst, R., Pardalos, P. M., Eds.; Kluwer Academic Publishers: Dordrecht, The Netherlands, 1997.
(17) Hansen, D. A.; Edgerton, E. S.; Hartsell, B. E.; Jansen, J. J.; Kandasamy, N.; Hidy, G. M.; Blanchard, C. L. The Southeastern Aerosol Research and Characterization Study: part 1—Overview. *J. Air Waste Manage. Assoc.* **2003**, *53*, 1460−1471.
(18) Kim, E.; Hopke, P. K.; Edgerton, E. S. Source identification of Atlanta aerosol by positive matrix factorization. *J. Air Waste Manage. Assoc.* **2003**, *53*, 731−739.
(19) Chow, J. C.; Watson, J. G.; Kuhns, H.; Etyemezian, V.; Lowenthal, D. H.; Crow, D.; Kohl, S. D.; Engelbrecht, J. P.; Green, M. C. Source profiles for industrial, mobile, and area sources in the Big Bend Regional Aerosol Visibility and Observational study. *Chemosphere* **2004**, *54*, 185−208.
(20) McDonald, J. D.; Zielinska, B.; Fujita, E. M.; Sagebiel, J. C.; Chow, J. C.; Watson, J. G. Emissions from charbroiling and grilling of chicken and beef. *J. Air Waste Manage. Assoc.* **2003**, *53*, 185−194.

(21) Zielinska, B.; McDonald, J. D.; Hayes, T.; Chow, J. C.; Fujita, E. M.; Watson, J. G. *Northern Front Range Air Quality Study Final Report. Volume B: Source Measurements*. http://www.nfraqs-.colostate.edu/nfraqs/index2.html.
(22) Cooper, J. A. *Determination of Source Contributions to Fine and Coarse Suspended Particulate Levels in Petersville, Alabama*. Report to Tennessee Valley Authority by NEA, Inc., 1981.
(23) Gillies, J. A.; Gertler, A. W. Comparison and evaluation of chemically speciated mobile source $PM_{2.5}$ particulate matter profiles. *J. Air Waste Manage. Assoc.* **2000**, *50*, 1459−1480.
(24) Unal, A.; Tian, D.; Hu, Y.; Russell, A. *2000 Emissions Inventory for Fall Line Air Quality Study (FAQS)*. Prepared for Georgia Department of Natural Resources, Environmental Protection Division, April 2003.
(25) Health Effects Institute (HEI). *Emissions from Diesel and Gasoline Engines Measured in Highway Tunnels*; Research Report 107; 2002.
(26) Marmur, A.; Mamane, Y. Comparison and evaluation of several mobile-source and line-source models in Israel. *Trans. Res. D.* **2003**, *8*, 249−265.
(27) Baek, J.; Russell, A. G. Private communication, 2004.

Received for review June 29, 2004. Revised manuscript received December 31, 2004. Accepted March 1, 2005.

ES0490121